Remodeling Capabilities of Synthetic High-Density Lipoprotein (sHDL) Nanoparticles: Influence of Lipid Composition, Acyl Chain Length, Charge, and Cholesterol Content

Sagar Dhakal
University of Helsinki
Faculty of Pharmacy

February 2026

Abstract

Faculty: Faculty of Pharmacy

Degree program: Master's programme in pharmaceutical research, development, and safety

Study track: Drug delivery and development

Author: Sagar Dhakal

Title: Remodeling Capabilities of Synthetic High-Density Lipoprotein (sHDL) Nanoparticles: Influence of Lipid Composition, Acyl Chain Length, Charge, and Cholesterol Content

Level: Master's degree

Month and year: February 2026

Number of pages: 38

Keywords: Apolipoprotein A-I mimetic peptides; synthetic high-density lipoprotein (sHDL); nanodisc; lipid-to-peptide ratio; remodeling; phase transition; atherosclerosis; macrophage foam cells

Supervisor or supervisors: Artturi Koivuniemi

Where deposited: University of Helsinki Library's digital archive HELDA

Additional information:

Abstract:

Atherosclerosis is a leading cause of mortality, and current therapies do not fully address residual cardiovascular risks associated with it. HDL-mediated reverse cholesterol transport (RCT) is a promising therapeutic target; however, therapies that increase HDL cholesterol levels have not consistently led to positive clinical outcomes. This highlights the need for innovative therapeutic approaches, such as synthetic HDL (sHDL) nanoparticles incorporating phospholipids and apoA-I mimetic peptides like 22A. While the peptide component of sHDL nanoparticles is well characterized, the impact of lipid composition on sHDL properties and remodeling efficacy is less understood. To address this, 12 distinct sHDL formulations containing 22A apoA-I mimetic peptide in combination with various phospholipids (DMPC, DPPC, DSPC), cholesterol, and the cationic lipid (DMTAP) were formulated at a 7:1 lipid-to-peptide molar ratio and systematically evaluated. The study aimed to investigate how lipid composition, acyl chain length, surface charge, and cholesterol content affect the morphology, size, phase transition behavior, and endogenous HDL remodeling capabilities of sHDL particles. Dynamic Light Scattering (DLS) revealed that lipid composition determined sHDL particle size, with significant differences among the formulations: DMPC-DPPC-22A produced the smallest (7.69 ± 2.03 nm), and DPPC-CHOL-22A yielded the largest (19.43 ± 6.69 nm) particles. Cryo-electron microscopy of DMPC-DMTAP-22A nanodiscs confirmed a disc-shaped morphology, characterized by circular top views and narrow, elongated edge-on profiles, with an average diameter of 19.01 ± 3.14 nm. Differential Scanning Calorimetry demonstrated that, unlike multilamellar vesicles, sHDL particles did not exhibit gel-to-liquid crystalline phase transitions. This observation might be explained by the peptide's constraining effect, the membrane's high curvature, and the coexistence of distinct core (gel-like) and boundary (liquid-disordered) lipid phases within the nanodisc. In vitro HDL remodeling assays showed that DMPC-22A, cholesterol-containing, and cationic lipid-containing sHDL nanoparticles induced extensive remodeling of endogenous HDL present in human plasma. These formulations significantly reduced α-HDL particles and increased lipid-poor apoA-I particles, as shown by gel electrophoresis followed by Western blotting with an anti-apoA-I antibody. In contrast, sHDL particles composed primarily of phospholipids with longer acyl chains (DPPC-22A, DSPC-22A) and a binary mixture of phospholipids (DMPC-DPPC, DPPC-DSPC, DSPC-DMPC) exhibited none to little remodeling, likely due to their core lipids remaining in a rigid, gel-like phase at physiological temperatures. Incorporation of

cholesterol enhanced remodeling in these less fluid nanodiscs, likely by altering lipid packing and fluidity. Furthermore, cationic lipid-containing nanodiscs extensively remodeled plasma HDL regardless of the primary phospholipid, highlighting the predominant role of electrostatic interactions in facilitating lipid and protein exchange, the mechanism by which remodeling interactions are thought to take place. Collectively, these findings establish a critical relationship between lipid composition, which in turn affects physical properties such as acyl chain length, phase transition, and charge, and remodeling capacity, providing critical guidance for the rational design of next-generation HDL mimetic therapeutics for atherosclerosis.

Contents

1. Introduction

Cardiovascular disease (CVD) remains the leading cause of mortality worldwide, responsible for approximately 32% of all annual deaths (Fan and Watanabe 2022). Atherosclerosis, a chronic inflammatory disorder marked by the accumulation of lipid-rich plaques within arterial walls, is the principal driver of many cardiovascular events, notably ischemic heart disease (IHD) and stroke. In Western societies, atherosclerosis is estimated to account for nearly 50% of CVD-related deaths (Pahwa and Jialal 2023). The pathogenesis of atherosclerosis initiates with endothelial dysfunction, triggered by factors such as hemodynamic stress, hypercholesterolemia, oxidative stress, apoptotic or necrotic debris, and metabolic disturbances such as hyperglycemia and hypoxia. This leads to endothelial activation, monocyte infiltration, internalization of LDL particles by macrophages, foam cell formation, local inflammation, and remodeling of the extracellular matrix, collectively contributing to the formation of atherosclerotic plaque (Kowara and Cudnoch-Jedrzejewska 2021; Ajoolabady et al. 2024). The formed plaque can ultimately rupture and lead to life-threatening events such as myocardial infarction and stroke. Risk factors for atherosclerosis include non-modifiable factors such as age, sex, and genetic predisposition, as well as modifiable risk factors such as tobacco smoking, physical inactivity, poor nutrition, high blood pressure, type-2 diabetes, dyslipidemia, and obesity (Poznyak et al. 2022). Other factors such as homocysteine, high-sensitivity C-reactive protein (hs-CRP), sleep disorders, sedentary lifestyle, air pollution, and environmental stress have also been identified as risk factors for atherosclerosis (Aprotosoaie et al. 2022).

Current approaches for treating atherosclerosis primarily focus on a combination of lifestyle modifications, pharmacological interventions, and revascularization procedures. Lifestyle changes, including smoking cessation, weight loss, dietary changes, increased physical activity, and stress management, are essential for reducing risk factors and preventing disease progression (van Trier et al. 2021). Pharmacological therapies typically include lipid-lowering agents such as statins, antihypertensive agents, antihyperglycemic medications, and antiplatelet therapies. Statins are the cornerstone

of lipid management, although their effectiveness can be limited by low oral bioavailability, water solubility, and adverse effects such as myotoxicity. Revascularization interventions such as coronary artery bypass grafting (CABG), percutaneous coronary intervention (PCI), and endarterectomy are commonly used to restore blood flow and alleviate symptoms in advanced cases of atherosclerosis (Hetherington and Totary-Jain 2022; Wang et al. 2025). Despite substantial reductions in low-density lipoprotein cholesterol (LDL-C) achieved with statins and other therapies, such as proprotein convertase subtilisin/kexin type 9 (PCSK9) inhibitors, a significant residual risk of atherosclerotic cardiovascular disease (ASCVD) persists. This residual risk highlights the limitations of current treatments that focus mainly on LDL-C reduction (Bashir et al. 2024). Consequently, novel therapeutic approaches such as those targeting reverse cholesterol transport (RCT) are required to further reduce cardiovascular risk and enhance patient outcomes (Ouimet et al. 2019).

RCT is a process by which HDL removes excess cholesterol from the peripheral tissues, including lipid-laden cells in the arterial wall, with the help of the ABC (ATP Binding Cassette) transporter family, mainly ABCG1 and ABCA1 in the macrophages, and scavenger receptor class B type I (SR-BI) in the hepatocytes, and delivers it to the liver for excretion through bile. High-density lipoprotein cholesterol (HDL-C) is the main lipoprotein involved in the RCT process (Marques et al. 2018). During RCT, HDL particles undergo remodeling, resulting in changes in their shape, size, and lipid composition, particularly cholesterol and phospholipids. This process is facilitated by enzymes such as lecithin-cholesterol acyltransferase (LCAT), cholesteryl ester transfer protein (CETP), and phospholipid transfer protein (PLTP) (Ouimet et al. 2019). Apolipoprotein A-I (apoA-I) is the major protein component of HDL and acts as a mediator of RCT by activating LCAT, an enzyme responsible for cholesterol esterification. Plasma levels of apoA-I are inversely associated with the risk of cardiovascular disease (Alexander et al. 2010). HDL is not only involved in RCT but also exerts antioxidant, anti-inflammatory, antithrombotic, cytoprotective, and endothelial-stabilizing effects (Casula et al. 2021). HDL promotes endothelial nitric oxide production and reduces LDL oxidation, thereby limiting the formation of foam cells. HDL also has enzymes such as paraoxonase (PON)

and platelet-activating factor acetylhydrolase (PAF-AH). These enzymes help to reduce oxidative stress and vascular inflammation (Bandeali and Farmer 2012). Despite the biological functions, pharmacological strategies aimed at increasing HDL-C levels, such as cholesteryl ester transfer protein (CETP) inhibitors, niacin, and fibrates, have not consistently reduced cardiovascular risk in patients treated with statins (Keene et al. 2014; Werba et al. 2019). These negative outcomes have led to the conclusion that the functionality of HDL particles is more important than HDL-C levels in plasma.

This led to the emergence of nanodiscs incorporating full-length apoA-I and phospholipids, such as ApoA-I Milano, a natural mutant variant of full-length apoA-I, and CER-001, a negatively charged, engineered pre-β HDL mimetic containing apolipoprotein A-I and sphingomyelin. These nanodiscs consisted of a lipid bilayer surrounded by a belt formed by amphipathic proteins, termed membrane scaffold protein (MSPs). MSPs are engineered derivatives from the human ApoA-I, which is a component of HDL particles (Wang and Tieleman 2024). However, the use of full-length or recombinant apoA-I has several limitations, including the potential for endotoxin/viral contamination, high production costs, variability in rHDL production, and lack of oral bioavailability (Nankar et al. 2022). Clinical trials have shown that infusing MDCO-216 (ApoA-I Milano) did not produce incremental plaque regression in the setting of contemporary statin therapy (Nicholls et al. 2018b), and infusing CER-001 did not promote regression of coronary atherosclerosis compared with placebo in statin-treated patients (Nicholls et al. 2018a). However, the clinical trials were conducted in patient populations that had already experienced a cardiovascular event requiring hospitalization. Consequently, the potential benefits of long-term treatment with HDL mimetics were not evaluated. The use of shorter apoA-I mimetic peptides, which replicate the amphipathic α-helical structure of apoA-I, would facilitate the design and implementation of such long-term clinical studies. Apolipoprotein mimetic peptides offer significant advantages over full-length apoA-I as they can be optimized for enhanced ABCA1-mediated cholesterol efflux, improved LCAT activation, superior antioxidant properties, reduced hemolytic potential, and increased stability, alongside being cost-efficient, safe, scalable, and flexible (Fawaz et al. 2020; Nankar et al. 2022). Some examples of apoA-I mimetic

peptides include 22A, 2F (18A), D-4F, L-4F, 5A, and ATI-5261. There has been substantial research dedicated to optimizing peptide sequences to enhance reverse cholesterol transport (Yuan et al. 2023). For example, attaching a proline residue to the 22A peptide was found to prevent its hydrolysis in plasma, improving its stability and circulation time (Fawaz et al. 2020). Alongside peptide optimization, the emergence of lipids such as POPC, DMPC, DPPC, DSPC, DMTAP, DMPG, and Sphingomyelin has prompted investigation into the impact of lipid content on particle stability, circulation time, and RCT (Miyazaki et al. 2013; Schwendeman et al. 2015). Variation in the composition of phospholipids has resulted in variation of pharmacokinetic and pharmacodynamic properties of synthetic high-density lipoprotein (sHDL) nanoparticles, which may be attributed to different phase transition temperatures seen in the particles (Rani and Marsche 2023).

This thesis investigates twelve distinct HDL mimetic sHDL particles prepared using DMPC, DPPC, DSPC, DMTAP, and Cholesterol in combination with 22A apoA-I mimetic peptide. The lipid content is varied in such a way that sHDL particles contain a single phospholipid, combination of two phospholipids, phospholipids with cholesterol, and phospholipid with cationic lipid (DMTAP), while maintaining a total lipid-to-peptide molar ratio of 7:1. The primary objective is to determine how the lipid composition, acyl chain length, charge and cholesterol content of sHDL particles influence their remodeling capabilities. Remodeling of endogenous HDL by sHDL particles is important, as recent research shows that HDL particles can be dysfunctional or even pro-inflammatory in atherosclerosis, and infusion of HDL mimetic nanoparticles restores the number and functionality of the native HDL (Rani and Marsche 2023; Madaudo et al. 2024). A secondary objective is to evaluate how variations in phospholipid composition affect the size and phase transition temperature of sHDL particles. The hypothesis of this study is that variation in the composition of phospholipids, including single and binary mixtures of lipids differing in acyl chain length and headgroup charge, as well as cholesterol content, influences the remodeling capacity of sHDL particles in plasma. This hypothesis is based on structural and functional information about phospholipids, such as the influence of chain length and cholesterol content on membrane fluidity. It is also

based on the fact that native HDL contains a net negative charge, and formulating sHDL particles with positively charged lipids may improve remodeling capacity by promoting fusion between native HDL and sHDL particles. Variations in lipid composition are likely to result in different structural organization and interaction with the peptide. Furthermore, the different mixtures of lipids are expected to influence the remodeling capacity by affecting the phase of lipids and configuration of 22A peptides in the rim of sHDL particles. Together, these investigations aim to provide a deeper understanding of compositional variation in the phospholipid content of sHDL particles and their influence on size, phase transition, and remodeling capability. These findings can be used as guidance for the rational design of future HDL mimetic therapeutics for atherosclerosis.

2. Materials and Methods

2.1. Materials

ApoA-I mimetic peptide 22A (PVLDLFRELLNELLEALKQKLK), further referred to as 22A, was obtained from Peptide Protein Research Ltd. (Fareham, UK). 1,2-dimyristoyl-sn-glycero-3-phosphocholine (DMPC), 1,2-dipalmitoyl-sn-glycero-3-phosphocholine (DPPC), 1,2-distearoyl-sn-glycero-3-phosphocholine (DSPC), and 1,2-dimyristoyl-3-trimethylammonium-propane chloride salt (DMTAP) were obtained from Avanti Polar Lipids Inc. (Alabaster, AL). Monoclonal anti-apoA-I antibody (clone 3A11-1A9, mouse), Cholesterol (≥ 99 %), Bovine serum albumin (heat shock fraction, pH 7, ≥ 98 %), Polyethylene glycol sorbitan monolaurate (Tween 20), and Sucrose (≥ 99.5 %) were obtained from Sigma-Aldrich (St. Louis, MO). Mini-Protean TGX Stain-Free Polyacrylamide gels 4 – 20 % (15-well comb, 15 µl), Trans-Blot Turbo Transfer Pack 0.2 µm nitrocellulose membrane, Native Sample Buffer, Coomassie Brilliant Blue R-250 Staining Solution were obtained from Bio-Rad (Hercules, CA). NativeMark HMW Protein Standards, Goat anti-mouse IgG secondary antibody HRP, SuperSignal™ west femto maximum sensitivity substrate were purchased from Thermo Fisher Scientific (Waltham, MA). Pooled human plasma from normal healthy donors was purchased from Innovative Research, Inc (Novi, MI).

2.2. Synthesis of sHDL nanoparticles

sHDL nanoparticles were prepared using the peptide 22A and various lipid compositions, including DMPC, DPPC, DSPC, cholesterol (CHOL), and DMTAP, resulting in twelve distinct formulations: DMPC-22A, DPPC-22A, DSPC-22A, DMPC:DPPC (1:1)-22A, DMPC:DSPC (1:1)-22A, DPPC:DSPC (1:1)-22A, DMPC:CHOL (3:1)-22A, DPPC:CHOL (3:1)-22A, DSPC:CHOL (3:1)-22A, DMPC:DMTAP (3:1)-22A, DPPC:DMTAP (3:1)-22A, and DSPC:DMTAP (3:1)-22A. The respective lipid combinations, dissolved in chloroform, were dried for 1 hour using a Rotavapor R-100 (BUCHI, Switzerland) at room temperature under 100 mbar to form a thin lipid film. The dried thin films were subsequently hydrated with 1X PBS pH 7.4 and homogenized via sonication in an ultrasonic bath (Elma Elmasonic S 40 H) at room temperature until the solution became clear, producing unilamellar vesicles. The appropriate volume of 22A peptide, dissolved in 1/50X PBS pH 7.4, was then added to achieve a fixed total lipid-to-peptide molar ratio of 7:1 for each combination of lipids. To facilitate sHDL self-assembly, the mixtures were subjected to three rounds of thermal cycling, alternating between 55°C (above T_m) and an ice bath (below T_m) for five minutes each. All synthesized nanodisc samples were stored at +4°C until further use.

2.3. sHDL Characterization with Dynamic Light Scattering

To assess the effect of lipid composition, charge, and cholesterol content on the size distribution of sHDL, twelve HDL mimetic nanodisc formulations – comprising 22A peptide and a phospholipid or mixture of phospholipids with or without CHOL were analysed using dynamic light scattering (DLS) with a Malvern Zetasizer APS at 25°C. The results are shown as the percentage volume distribution of hydrodynamic diameters. Data are represented as the average value of three measurements.

2.4. sHDL Characterization with Cryo-Electron Microscopy

To examine the morphology of formed sHDL particles, one representative formulation composed of DMPC-DMTAP-22A was selected for characterization using cryo-electron microscopy (cryo-EM) on a Talos Arctica instrument equipped with a Falcon 4i camera at 200 kV. The sample was prepared at a concentration of 0.2 mg/ml (peptide basis) in

1X PBS pH 7.4. Quantifoil grids were rendered hydrophilic by glow discharge, and 3 µL of sample was applied onto the grid surface, followed by 10 seconds of preblotting and 1.5 seconds of blotting step to remove excess liquid using a filter paper. Grids were vitrified by rapid plunging into liquid ethane using a Leica EM GP2 vitrification system and subsequently stored in liquid nitrogen until imaging. The grids were clipped, and Cryo-EM data were collected with a total electron dose of 41.65 e/Å², a dose rate of 11.39 e/px/s, and an exposure time of 3.11 s, resulting in a pixel size of 0.92 Å. Images were acquired from different regions of the grid after visually screening the grid to identify areas with well-vitrified ice to obtain image with good quality. Particles were selected manually by eye. Particle diameter and thickness were measured manually using ImageJ, and the average size and standard deviation were calculated from these measurements.

2.5. Differential Scanning Calorimetry

The phase transition temperature (T_m) of the prepared sHDL particles was assessed using differential scanning calorimetry (DSC, TA DSC250, TA Instruments, New Castle, United States). Prior to measurement, the sHDL particles were freeze-dried, reconstituted in Milli-Q water to obtain a lipid concentration of 20 mM, and subjected to three freeze–thaw cycles to ensure homogeneity. For analysis, 20 µL of the sample was pipetted into a Tzero aluminum pan (TA Instruments, Switzerland) and sealed with a Tzero hermetic lid in which a small hole was introduced to allow pressure release. The reference pan was left empty, while the sample pan contained the sHDL particles. Thermal scans were carried out under a nitrogen atmosphere using a linear heating rate of 5 °C per minute (DMPC-22A nanodiscs) and 1 °C per minute (DMPC-22A & DSPC-22A nanodiscs) over a temperature range of 10 to 90 °C, adjusted according to the lipid composition. In addition to the nanodisc samples, multilamellar vesicles (MLVs) in 1X PBS prepared without peptides were also analyzed as controls to verify the accuracy and reliability of the experimental setup. The phase transitions were identified as characteristic endothermic peaks and processed using TRIOS software (TA Instruments, New Castle) and Microsoft Excel.

2.6. Remodeling of endogenous HDL by sHDL nanoparticles

Human plasma was incubated with 1X PBS (control) and sHDL particles at a final peptide concentration of 1 mg/mL for 1 hour at 37 °C. Reactions were terminated by a 10-fold dilution with a 50 % w/v sucrose solution. The diluted samples were mixed in equal volumes with loading buffer, and 10 µL of each mixture, along with 10 µL of NativeMark HMW protein standards, were applied to a 4–20% polyacrylamide gel pre-equilibrated in 25 mM Tris, 1.92 M glycine, pH 8.3. Electrophoresis was performed for 2 hours at 200 V. The molecular weight ladder lane was excised and stained with Coomassie, while the remaining gel was transferred to a 0.2 µm nitrocellulose membrane using the Bio-Rad Trans-Blot Turbo system (10 minutes, 1.3 A). The membrane was blocked for 1 hour in 5% BSA in TBST (20 mM Tris, 150 mM NaCl, 0.1% Tween-20, pH 7.6). Overnight incubation at 4 °C was performed with a monoclonal anti-apoA-I antibody (mouse; 1:3000 dilution; stock 0.2 mg/mL) prepared in 5% BSA in TBST. After primary incubation, the membrane was washed three times with 1X TBST for 10 minutes each. The blot was then incubated for 1.5 hours with a goat anti-mouse IgG HRP-conjugated secondary antibody (1:7000 dilution; stock 1.5 mg/mL) in 5% BSA in TBST. Following this, the membrane was again washed three times with 1X TBST for 10 minutes each. The blot was exposed to an enhanced chemiluminescent reagent for 5 minutes and imaged using the Bio-Rad ChemiDoc MP system. Protein standards included apoferritin (480 kDa, 12.2 nm), B-phycoerythrin (242 kDa, 10.1 nm), lactate dehydrogenase (146 kDa, 8.1 nm), and BSA (66 kDa, 7.1 nm) (Gantt 1969; Yohannes et al. 2010; Cascajo-Castresana et al. 2020; Pasti et al. 2022). The anti-apoA-I antibody was confirmed not to recognize the 22A peptide. The assay was performed in triplicate using 12 different sHDL formulations, with plasma used as the control.

2.7. Statistical Analysis

Data are represented as mean ± standard deviation (SD) of triplicate measurements. Statistical analysis was performed using IBM SPSS Statistics, and figures were generated using Microsoft Excel and BioRender.com.

3. Results

3.1. Preparation and Characterization of sHDL particles with Dynamic Light Scattering

DLS was used to characterize the size distributions of 12 HDL-mimetic nanodisc formulations, enabling evaluation of how lipid composition, acyl chain length, surface charge, and cholesterol content affect nanoparticle morphology. The hydrodynamic radius and polydispersity index (PDI) were determined for nanodiscs composed of a single phospholipid, a mixture of phospholipids, phospholipid–cholesterol combinations, and assemblies containing both neutral and positively charged phospholipids with the 22A peptide at a 7:1 lipid-to-peptide molar ratio (Figure 1).

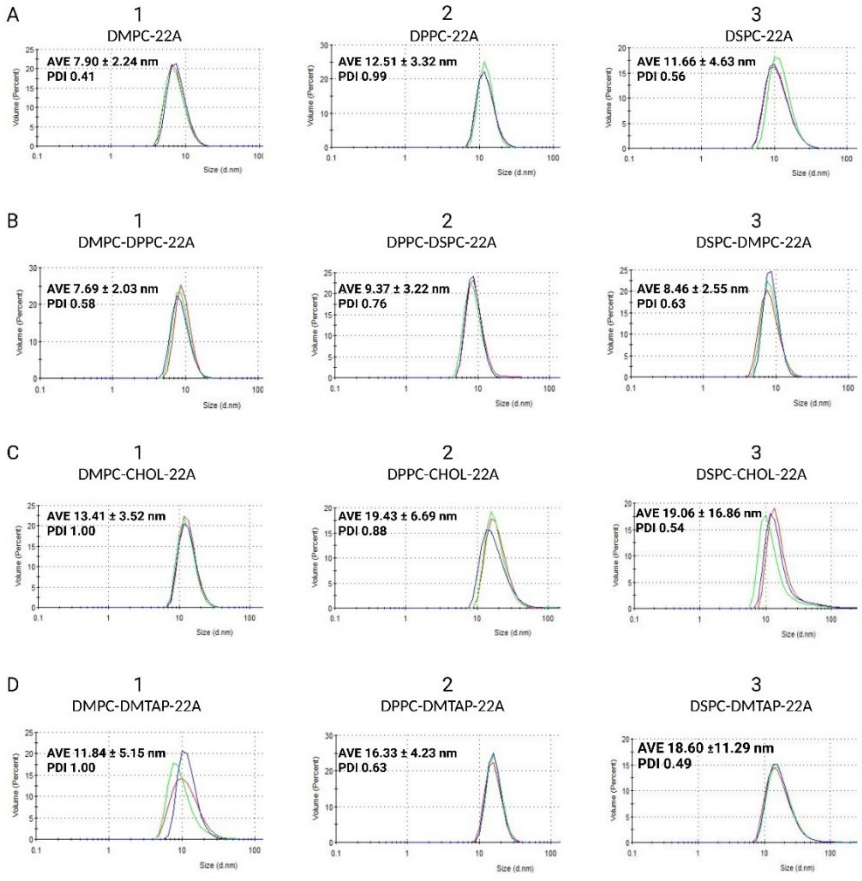

Figure 1: Size distribution by volume of sHDL particles containing 22A peptide measured with dynamic light scattering. sHDL particles with single phospholipid (A); sHDL particles with a binary mixture of phospholipids (B); sHDL particles with a phospholipid and cholesterol (C); sHDL particles with a neutral phospholipid and cationic lipid (D).

Among the single-phospholipid formulations, the smallest sHDL particle was observed for DMPC-22A (7.90 ± 2.24 nm). In contrast, for mixed-phospholipid systems, DMPC-DPPC-22A exhibited the smallest particle size (7.69 ± 2.03 nm). The smallest nanodiscs incorporating cholesterol and phospholipids were observed for DMPC-CHOL-22A (13.41 ± 3.52 nm), whereas those containing both neutral and cationic lipids showed the smallest size for DMPC-DMTAP-22A (11.84 ± 5.15 nm). Overall, the smallest sHDL particles were obtained with DMPC-DPPC-22A (7.69 ± 2.03 nm), while the largest were observed for DPPC-CHOL-22A (19.43 ± 6.69 nm). The PDI values ranged from 0.41 to 1.00, indicating notable heterogeneity in size distribution across different nanodisc formulations. More than 95% of the volume-weighted size distribution corresponded to nanodisc-sized particles, while a minor fraction consisted of larger particles. Table 1 summarizes the hydrodynamic diameters of the sHDL particles, measured by DLS using percentage volume distribution.

Table 1: Percentage volume distribution (hydrodynamic diameters) of different sHDL formulations

Formulation	Lipid(s)	Peptide	Lipid to peptide ratio (molar)	Size (d,nm)
Single phospholipid	DMPC	22A	7:1	7.90 ± 2.24
	DPPC			12.51 ± 3.32
	DSPC			11.66 ± 4.63
Binary phospholipids	DMPC-DPPC (1:1)		7:1	7.69 ± 2.03
	DPPC-DSPC (1:1)			9.37 ± 3.22
	DSPC-DMPC (1:1)			8.46 ± 2.55
Phospholipid + Cholesterol	DMPC-CHOL (3:1)		7:1	13.41 ± 3.52
	DPPC-CHOL (3:1)			19.43 ± 4.69
	DSPC-CHOL (3:1)			19.06 ± 16.86
Phospholipid + Cationic lipid	DMPC-DMTAP (3:1)		7:1	11.84 ± 5.15
	DPPC-DMTAP (3:1)			16.33 ± 4.23
	DSPC-DMTAP (3:1)			18.60 ± 11.29

When the hydrodynamic diameters of sHDL nanoparticles were examined in relation to phospholipid acyl chain length, a clear relationship was observed between them. The data revealed that particle size increases with phospholipid fatty acyl chain length, as illustrated in Figure 2.

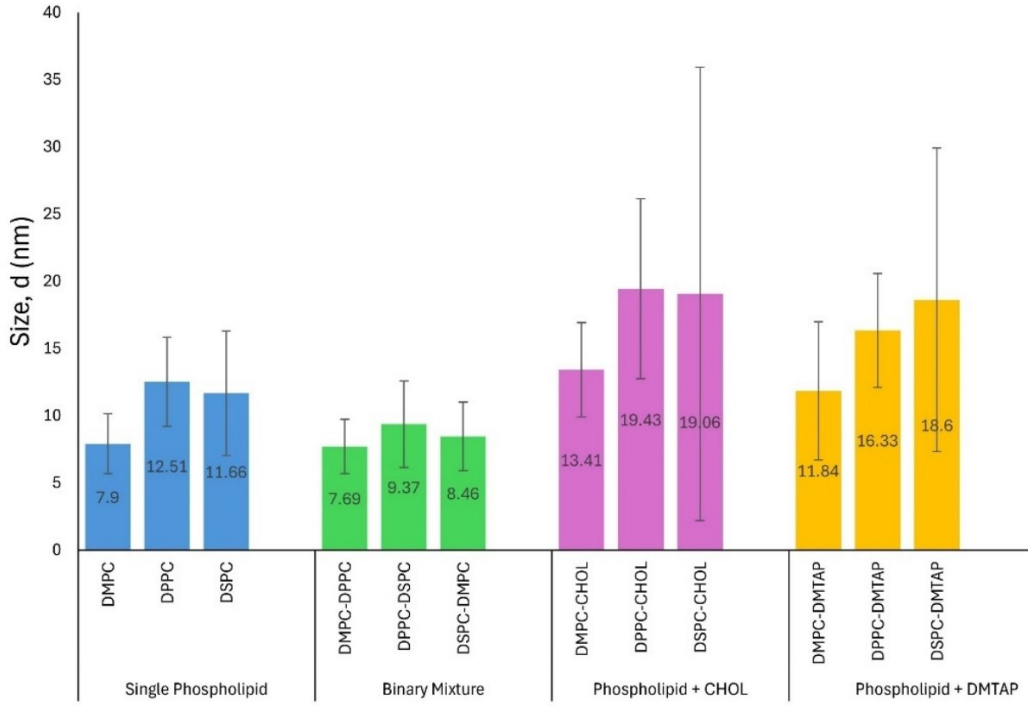

Figure 2: Size of 22A-sHDL particles as a function of acyl chain length. Hydrodynamic diameters were measured by DLS using percentage volume distribution for four formulation groups: single phospholipids, binary phospholipid mixtures, phospholipids with cholesterol, and phospholipids with DMTAP. The data show that the size of 22A-sHDL particles generally increases with increasing phospholipid fatty acyl chain length.

3.2. Characterization of sHDL particles with Cryo-Electron Microscopy

Cryo-EM was employed to access the morphology and size of DMPC-DMTAP-22A nanoparticles prepared at a total lipid-to-peptide molar ratio of 7:1. Cryo-EM micrographs revealed particles exhibiting morphology consistent with nanodiscs. The particles appeared circular in top view, whereas in edge-on views, they were narrow and elongated, with a certain thickness. Quantitative particle size analysis was performed on Cryo-EM micrographs using ImageJ, and the resulting data were compared to hydrodynamic diameters obtained from DLS measurements (Figure 2). Cryo-EM analysis

indicated an average particle diameter of 19.01 ± 3.14 nm, for which the corresponding DLS-derived hydrodynamic diameter was 11.84 ± 5.15 nm. The bilayer thickness was 5.76 nm as calculated by ImageJ.

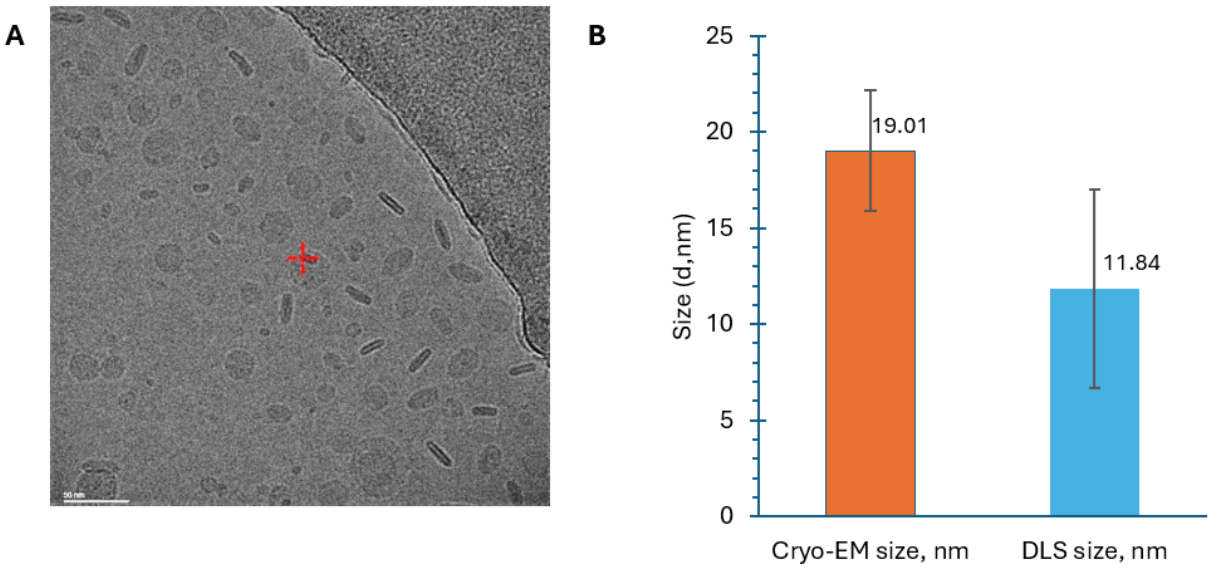

Figure 3: Cryo-EM micrograph (A), and volume-based DLS particle size distribution compared with Cryo-EM measurements for DMPC-DMTAP-22A particles. The scale bar of the cryo-EM image is 50 nm. Mean particle diameter and standard deviation measured by cryo-EM (orange bar) and DLS size distribution by volume (blue bar). DLS experiments were conducted at 25 °C. Values above bars indicate mean ± SD in nm.

3.3 Differential Scanning Calorimetry

Differential scanning calorimetry (DSC) is a highly sensitive, non-perturbing technique that measures the heat energy difference between a sample and reference during a controlled temperature change. It is an effective tool for studying the thermotropic properties of protein–lipid interactions and lipid bilayer phase transitions (Cañ and Casals 2013; Durowoju et al. 2017). Previous studies on DMPC-MSP and DPPC-MSP nanodiscs have reported broader phase transitions than those observed in liposomes. The presence of the membrane scaffold protein (MSP) around the lipid bilayer alters lipid packing, resulting in a less cooperative transition (Johansen et al. 2021). For example, the phase transition temperature for DMPC-based nanodiscs was approximately 28.5 °C, whereas for DPPC-based nanodiscs it was around 44.5 °C (Denisov et al. 2005). In this study, we investigated the phase transition behaviour of

nanodiscs formed with 22A apoA-I mimetic peptide in combination with various lipid formulations. The nanodiscs were prepared at a final lipid concentration of 20 mM and analyzed using DSC 250. The sample pan contained the reconstituted nanodiscs, while the reference pan was left empty. The experiment was conducted over a temperature range of 10 to 70°C, with a heating rate of 5 °C per minute for DMPC-22A nanodiscs and 1 °C per minute for DMPC-22A & DSPC-22A nanodiscs. MLVs, prepared without peptides at the same lipid concentration (20 mM), served as a control. The nanodiscs formed with DMPC, DPPC, and DSPC did not exhibit distinct phase transitions in their DSC thermograms, whereas the MLVs did exhibit clear phase transitions (Figure 3). For DMPC MLVs, the onset of transition occurred at 21.77 °C; for DPPC at 40.16 °C; and for DSPC at 52.71 °C, which are near the reported values for these lipids. Since these nanodiscs did not exhibit phase transitions, DSC measurements of other nanodiscs with different compositions of lipids were not carried out. The resulting thermograms were expressed as Heat Flow (Normalized) Q (W/g) vs Temperature (°C).

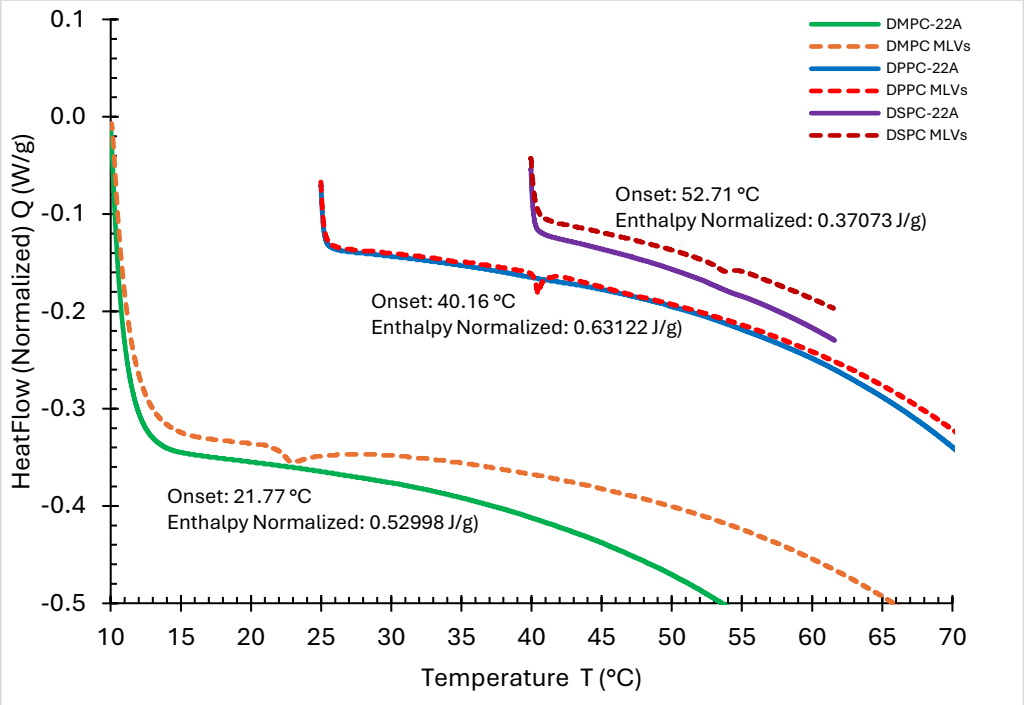

Figure 4: Differential scanning calorimetry (DSC) scans of DMPC-22A, DPPC-22A, and DSPC-22A nanodiscs, presented as normalized heat flow Q(W/g) as a function of temperature (°C). The onset temperature and normalized enthalpy values are indicated in the figure. The scans for nanodiscs are represented by solid lines, while those for MLVs are shown as dotted lines.

3.4. Remodeling effect of sHDL particles on Human Plasma

HDL is a heterogeneous population of particles that vary in size, shape, protein and lipid composition, and may be crucial in differentially modulating cholesterol efflux and RCT (Ronsein and Vaisar 2017). These particles can be categorized into lipid-poor apoA-I, pre-β HDL, and α-HDL. Lipid-poor apoA-I particles are released into the plasma from the liver or intestine, and these small, dense particles have the highest capacity to induce cholesterol efflux from macrophages, initiating the RCT process (Zhao et al. 2013; Trajkovska and Topuzovska 2017). Lipid-poor apoA-I particles absorb phospholipids and cholesterol from cell membranes and other lipoproteins, transitioning into discoidal pre-β HDL particles. These discoidal particles serve as substrates for lecithin-cholesterol acyltransferase (LCAT), which esterifies cholesterol, converting it into spherical α-HDL, the predominant form of HDL in plasma. The spherical shape results from the migration of cholesteryl esters (CEs) into the middle of phospholipid leaflets and forms a hydrophobic core when the concentration of CEs is high enough (Rye et al. 2009; Phillips 2013; Ouimet et al. 2019). sHDL particles, such as those containing full-length apoA-I or mimetic peptides, are thought to remodel endogenous α-HDL particles by fusing with them, leading to an increase in discoidal pre-β HDL and lipid-poor apoA-I particles. Lipid and protein exchange between sHDL and endogenous HDL particles may contribute to remodeling. In this study, we investigated the ability of sHDL particles composed of the 22A apoA-I mimetic peptide in combination with various lipid formulations to remodel endogenous HDL in human plasma. Remodeling was assessed by evaluating changes in the distribution of these HDL subfractions, with a decrease in α-HDL, an increase in pre-β HDL, and an increase in lipid-poor apoA-I particles, indicating successful remodeling. The plasma sample treated with 1X PBS (control) contained mainly mature α-HDL particles. We observed that DMPC-22A nanodiscs, cholesterol-containing nanodiscs, and cationic lipid-containing nanodiscs induced the greatest remodeling of endogenous HDL (Figure 5). These formulations caused a substantial decrease in α-HDL particles, accompanied by a slight increase in pre-β HDL and a substantial increase in lipid-poor apoA-I particles. On the other hand, formulations such as DPPC-22A, DMPC-DPPC-22A, DPPC-DSPC-22A, and DSPC-DMPC-22A did not seem to significantly alter the distribution

of HDL subfractions. These formulations showed only minor reductions in α-HDL levels and a slight increase in pre-β HDL and lipid-poor apoA-I. Additionally, DSPC-22A did not appear to induce any significant remodeling of endogenous HDL, as no substantial changes were observed in the HDL subfractions.

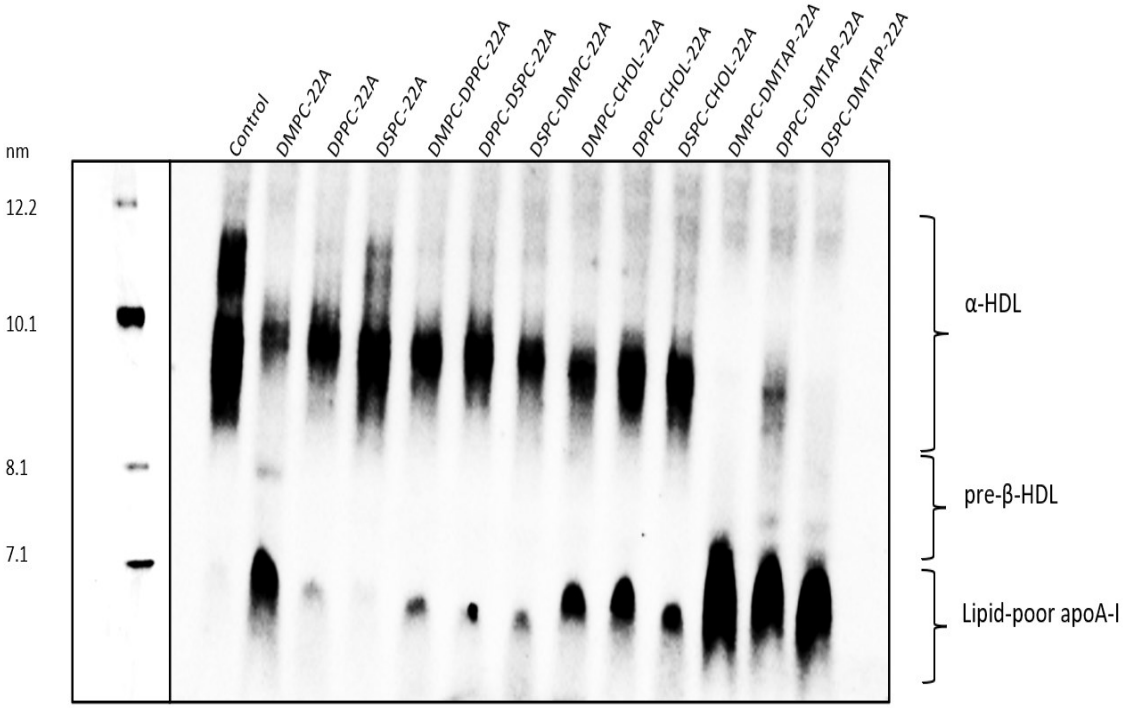

Figure 5: Remodeling of endogenous HDL in human plasma by sHDL particles. Plasma samples were incubated with different sHDL particles containing 22A peptide for 1 hour at 37 °C. Lipoproteins were separated by nondenaturing polyacrylamide gradient gel electrophoresis followed by Western blotting with an anti-apoA-I antibody.

To assess the specificity of the anti-apoA-I antibody and ensure that the observed bands did not result from binding to the peptide or nanodiscs, the 22A peptide and DMPC–DMTAP nanodiscs were each incubated in 1× PBS and in human plasma for 1 h at 37 °C. No signal was detected for either the 22A peptide or the DMPC–DMTAP nanodiscs under PBS conditions (Figure 5), confirming the specificity of the anti-apoA-I antibody. In contrast, incubation in plasma resulted in the appearance of lipid-poor apoA-I, with visually similar band intensities in both formulations.

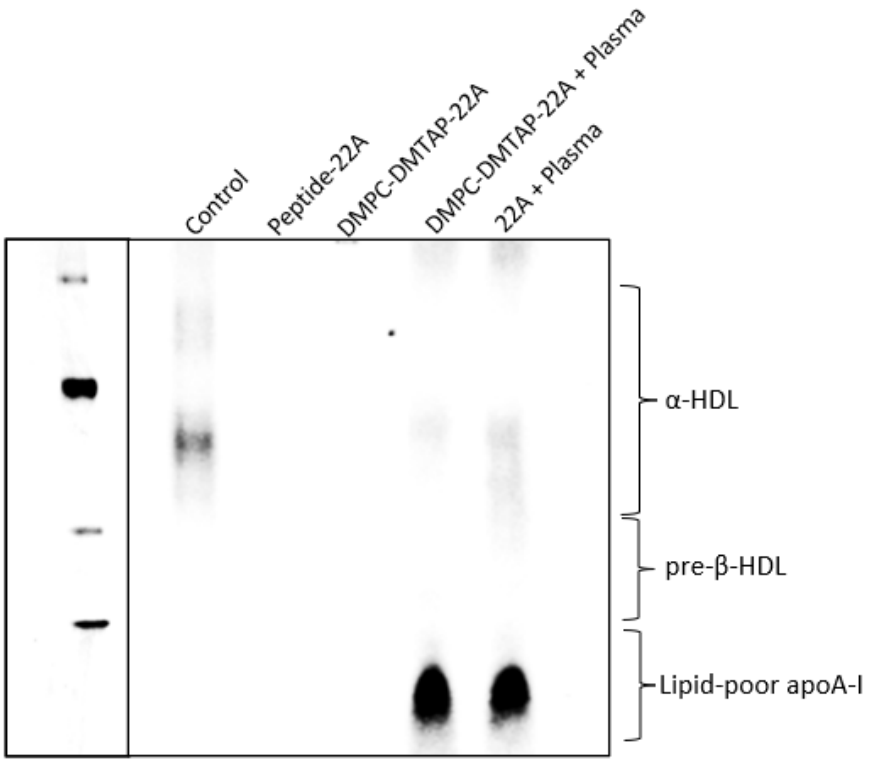

Figure 6: Specificity of the anti-apoA-I antibody used in our study. 22A peptide and DMPC-DMTAP-22A nanodiscs were incubated with 1 X PBS (Lane 2 and 3) and Plasma (Lane 5 and 4) for 1 hour at 37 °C. Electrophoresis followed by Western blotting with an anti-apoA-I antibody revealed no binding to the 22A peptide alone or to DMPC-DMTAP-22A nanodiscs alone.

4. Discussion

ASCVD remains the leading cause of mortality and morbidity globally (Mahmood and Shapiro 2021). Despite lowering LDL-C to very low levels, significant residual risk persists with currently used therapies such as statins and PCSK9 inhibitors (Riaz et al. 2019). In the meantime, therapies such as MDCO-216 (ApoA-I Milano) did not produce incremental plaque regression, and CER-001 did not promote regression of coronary atherosclerosis (Nicholls et al. 2018b, a). Furthermore, the use of full-length apoA-I has limitations such as potential for endotoxin/viral contamination, high production costs, variability in rHDL production, and lack of oral bioavailability (Nankar et al. 2022). These limitations have led to the emergence of sHDL nanoparticles composed of phospholipids and apoA-I mimetic peptides such as 22A. While significant research has been conducted to optimize the peptide component of sHDL particles, optimizing the lipid component is

equally important for cholesterol efflux from macrophages, interaction with LCAT, and cholesterol mobilization in vivo (Fawaz et al. 2020).

This study systematically investigates how variation in the composition of phospholipids, acyl chain length, cholesterol content, and the charge of sHDL particles governs the size, phase transition, and the ability to remodel native HDL. Twelve distinct formulations were made with 22A peptide at the total lipid-to-peptide molar ratio of 7:1 (2:1 weight ratio) varying the lipid component such that the formulation contained single phospholipid, a combination of phospholipids (1:1), phospholipid with cholesterol (3:1) and phospholipid with cationic lipid (3:1). The research aims to explore and answer two major research questions: (1) How do properties of sHDL nanoparticles such as size, phase transition vary with lipid composition? (2) How do the composition, acyl chain length, cholesterol content, and charge affect the remodeling capabilities of sHDL nanoparticles on native HDL?

The underlying hypothesis was that variation in the composition of phospholipids and cholesterol alters effective acyl chain length, fluidity, and charge, which in turn influences the size, morphology, phase transition, and remodeling capability of sHDL particles. This hypothesis is based on the structural and functional properties of phospholipids and on previous research findings on the effects of cholesterol and charge on membrane fluidity and remodeling (REF). Puthenveetil et al. (2016) constructed computational nanodisc models using the nanodisc builder from CHARMM GUI with lipids differing in acyl chain length, such as DMPC (14:0), DPPC (16:0), POPC (16:0- 18:1), and DSPC (18:0), and demonstrated that acyl chain length affects the thickness of the lipid bilayer. They observed that DMPC with the shortest acyl chain formed the thinnest nanodiscs with a bilayer thickness of 2.5 nm, while DSPC, with the longest acyl chain, produced the thickest nanodiscs with a bilayer thickness of 3.2 nm. Similarly, findings from You et al. (2022) suggest that lipid composition can be adapted to tune the membrane surface properties by varying the relative abundance of lipid classes with distinct intrinsic headgroup size, polarity, H-bonding ability, and surface charge. These properties strongly impact interfacial structure and dynamics, and hence the size of the discs formed. Research findings indicate that cholesterol governs membrane properties,

including thickness, fluidity, and permeability (Khodadadi et al. 2025). Cholesterol has a condensing effect and increases the bending rigidity of saturated lipid membranes (Chakraborty et al. 2020). The native HDL particles exhibit a net negative charge (Sparks et al. 2008), and formulating sHDL particles with positively charged lipids such as DMTAP may improve remodeling capacity by promoting fusion between native HDL and sHDL particles. Furthermore, the acyl chain length of phospholipids and cholesterol content in nanodiscs is expected to influence the remodeling capacity by affecting the phase behaviour of lipids and configuration of 22A peptide, which arranges itself in the rim of nanodiscs (Fawaz et al. 2020; Schachter et al. 2022; Khodadadi et al. 2025). Fawaz et al. (2020) observed a progressive decrease in endogenous HDL remodeling efficiency for 22A-sHDL particles prepared with phospholipids of increasing acyl-chain length, namely DMPC, DPPC, and DSPC. These research findings align with our hypothesis, and this investigation aims to provide a deeper understanding of compositional variation and charge-dependent properties of sHDL particles on remodeling native HDL.

Peptide 22A, also known as ESP24218, or ETC-642 (when complexed with sphingomyelin and DPPC), was selected in this research to study the remodeling capabilities of sHDL particles, as this 22-amino acid containing synthetic peptide is an amphipathic apolipoprotein A-I mimetic peptide. It was originally engineered to replicate the critical amphipathic α-helical structure of native ApoA-I when combined with lipids (Di Bartolo et al. 2011). Peptide 22A is specifically optimized to facilitate the interaction of peptide-based sHDL with lecithin-cholesterol acyltransferase (Yuan et al. 2023). Furthermore, 22A has advanced into human clinical development. It was the first ApoA-I mimetic peptide to reach this stage, where it was administered as ETC-642 in both single and multiple-dose trials. The development of ETC-642 was terminated in 2006, despite being considered safe and well-tolerated at all tested dose levels (Bourdi et al. 2018). DMPC, DPPC, and DSPC were chosen for the formulation of sHDL particles because they are saturated phospholipids differing in fatty acid chain length and, consequently, distinct phase transition temperatures. DMPC has 14 carbon chains, DPPC has 16, and DSPC has 18. Cholesterol was included in the research to examine its role in modulating nanodisc properties through its effect on lipid fluidity, packing, and phase transitions. Similarly,

DMTAP was included because it is a positively charged lipid and might affect the remodeling capability of formulated sHDL particles by promoting fusion with endogenous HDL in plasma via charge-charge attraction. A lipid-to-peptide molar ratio of 7:1 or a weight ratio of 2:1 was chosen to formulate the sHDL particles, as this ratio has been well established by several studies to produce homogeneous, stable, and functionally optimized nanodiscs. Tang et al. (2017) demonstrated that a 2:1 weight ratio of phospholipid to 22A peptide results in the formation of homogeneous HDLs with diameters ranging from 10 to 12 nm. Subsequent research by Kuai et al. (2017), Yu et al. (2022) and Kim et al. (2023) corroborates this finding and states that the optimal weight ratio of phospholipid-to-peptide to result in homogenous preβ-HDL like nanodisc is 2:1. Kleinauskaite (2025) prepared 12 different nanodiscs at various peptide-to-lipid molar ratios (1:5, 1:7, 1:10) using DMPC and peptides 22A, 22A-L14C, 22A-F23, 22A-P-18A and concluded that the 1:7 peptide-to-lipid molar ratio produced the smallest and the most uniform nanodiscs as indicated by lower size distribution and polydispersity index. These findings firmly establish the 7:1 lipid-to-peptide molar ratio as a well-justified choice for the assembly of stable, monodisperse nanodisc systems. In the future, it would be valuable to investigate how the lipid-to-peptide ratio and the use of different peptides influence the remodeling of endogenous HDL particles.

Among the formulations containing a single phospholipid, DMPC yielded the smallest sHDL particles (7.90 ± 2.24 nm), followed by DPPC (12.51 ± 3.32 nm) and DSPC (11.66 ± 4.63 nm). The observed differences in size (d, nm) may be attributed to differences in the fatty acyl chain lengths of phospholipids. DMPC has the shortest fatty acyl chain (C14) compared to DPPC (C16) and DSPC (C18). Phospholipids with long, saturated fatty acid chains are very tightly packed, and the chains become straighter and more ordered, increasing the bilayer thickness (Drabik et al. 2020). It can be noted that, despite having a shorter acyl chain length (C16) than DSPC (C18), DPPC formed slightly larger sHDL particles. This finding may be explained by intrinsic properties of lipid, such as area per lipid (APL) and bending rigidity (κ). DPPC exhibits a higher APL (50.9 ± 0.2 Å²) and a higher bending rigidity (4.28×10^{-20} J) compared to DSPC, which has an APL of 49.7 ± 0.2 Å² and a bending rigidity of 3.74×10^{-20} J (Hartkamp et al. 2016; Drabik et al. 2020). Higher APL

and bending rigidity of the DPPC bilayer when compared to DSPC suggest that lipids are loosely bound and require more energy to bend, resulting in larger discs despite their smaller fatty acyl chains. DMPC bilayers exhibit lower bending rigidity and a higher APL, reflecting a more disordered and thinner bilayer that is easier to bend, thus forming the smallest sHDL particles. Formulations employing two phospholipids in a 1:1 molar ratio produced particles of similar or slightly smaller size than those from single phospholipids. This suggests that the physical properties of combined phospholipids can optimize packing or curvature, potentially influencing self-assembly. Incorporation of cholesterol led to a notable increase in the size of sHDL particles with DMPC-CHOL, DPPC-CHOL, and DSPC-CHOL, exhibiting larger diameters compared to their cholesterol-free sHDL counterparts. This finding is consistent with the results obtained by Jakubec et al. (2021), in which the incorporation of 30 % w/w cholesterol into DOPC nanodiscs caused a significant increase in the mean size from 10 nm to 32 nm. The Increase in nanodisc size upon addition of cholesterol may be due to cholesterol insertion into the bilayer, which interacts with the hydrophobic chains of phospholipids, causing them to straighten and to induce greater orientational order of the bilayer (Sparr et al. 2002; Pan et al. 2008). Cholesterol is also known to cause thickening, condensing, and strengthening of the bilayer (Hung et al. 2007; Lyu et al. 2020). This might result in nanodiscs containing cholesterol adopting a larger diameter. The addition of the cationic lipid DMTAP to zwitterionic DMPC, DPPC, or DSPC resulted in larger sHDL particles than those prepared with single or binary phospholipids. Electrostatic interactions between the positively charged head group of DMTAP, the zwitterionic PC headgroups, and the 22A peptide might alter the peptide-lipid self-assembly process and stability. Wadsäter et al. (2013) demonstrated that anionic DMPG results in stable nanodiscs across various concentrations, whereas anionic DMPA and cationic DMTAP exhibit limited formation and stability with MSP1D1. These findings suggest that electrostatic interactions might influence the formation, size, and stability of nanodiscs. Among the twelve different sHDL formulations evaluated, the DMPC–DMTAP–22A formulation was selected for cryo-electron microscopy analysis. A comparison of the average particle size obtained by cryo-EM and DLS revealed differences between the two techniques. Cryo-EM analysis

yielded an average particle diameter of 19.01 ± 3.14 nm, whereas DLS measurements indicated a smaller mean hydrodynamic diameter of 11.84 ± 5.15 nm. The reason for such variation may arise from differences in nanodisc behaviour in solution compared with vitrified ice, as well as from the significant differences in the number of particles analyzed using each technique. In addition, DLS assumes that particles are spherical; therefore, when discoidal particles are analyzed, the reported size represents an averaged value. Furthermore, the diameters obtained from cryo-EM were measured from the top views, and the thickness was measured from the side views of the nanodiscs.

Analysis of phase transition behaviour of sHDL particles formed using 22A apoA-I mimetic peptide with phospholipids of varying acyl chain lengths (DMPC, DPPC, DSPC) revealed clear differences when compared to multilamellar vesicles (MLVs). The MLVs consisted of a single phospholipid species and were devoid of peptide, whereas both the nanodiscs and MLVs contained a total lipid concentration of 20 mM. Despite having the same lipid content, the sHDL particles did not exhibit a sharp gel-to-liquid-crystalline phase transition, whereas the MLVs displayed well-defined transition temperatures, as indicated by the endothermic peaks in the DSC thermograms. The measured phase transition temperature of MLVs (DMPC: 21.77 °C, DPPC: 40.16 °C, DSPC: 52.71 °C) align closely with the reported values in the literature (Mabrey and Sturtevant 1976). These transitions reflect the cooperative melting of lipid acyl chains from a rigid, ordered gel phase below T_m to a disordered fluid crystalline phase near or above T_m (Chen et al. 2018). Nanodiscs are nanoscale assemblies with a diameter in the order of ~10 nm, which introduce pronounced curvature effects, which are minimal or negligible in the case of MLVs. Experimental studies on pure DPPC vesicles have demonstrated that the phase transition temperature decreases as the vesicle diameter is reduced below ~ 70 nm, an effect attributed to inefficient lipid packing in highly curved membranes (Risselda and Marrink 2009). In nanodiscs, the curvature effect might be further compounded by the incorporation of the 22A apoA-I mimetic peptide, which disrupts long-range lipid packing and introduces a structural constraint by forming a double belt, picket fence, or random configuration around the lipid bilayer in an antiparallel head-to-tail fashion

(Krishnarjuna et al. 2025; Nouri et al. 2025). The formation of sHDL particles is temperature-dependent, occurring spontaneously at temperatures near or above the phospholipid T_m, suggesting that lipids must be in a liquid-disordered state to fully interact with peptides and form stable nanodisc structures (Patel et al. 2019). This suggests that sHDL particles may maintain this liquid-disordered state across a wide range of temperatures, thereby abolishing the gel-to-fluid phase transition. This interpretation is further supported by the work of Martinez et al. (2017), who reported that nanodiscs lack a well-defined gel-to-fluid phase transition and maintain lipid fluidity over a broad range of temperatures. Their study showed that DMPC liposomes were in the gel phase below 20 °C, with very tight packing; however, lipids in nanodiscs exhibited axially symmetric motions, and, even at temperatures significantly below T_m, a mixture of fluid and gel-like phases are present. Stepien et al. (2020) demonstrated the presence of core and boundary lipids in nanodiscs. The central lipids are highly ordered, exhibit slow diffusion, and are present in a gel-like or liquid-ordered phase. In contrast, the boundary lipids, which are in direct contact with the scaffold protein, are less ordered, have faster diffusion, and remain in a liquid disordered phase even at temperatures below T_m. Molecular dynamics simulation of DPPC nanodiscs by López et al. (2019) showed a gel-like domain in the central region, whereas the nanodisc rim remained in a fluid, disordered state. Thus, smaller size, high curvature, the constraining effect of peptide 22A, and the presence of two phases simultaneously within the nanodisc might prevent the propagation of a collective phase transition from the boundary to the core, thereby abolishing the gel-to-fluid phase transition.

Our experimental results demonstrate a link between these unique phase properties of nanodiscs and their ability to remodel native HDL in plasma. We observed that nanodiscs composed of binary phospholipids remodeled plasma HDL to a lesser extent, whereas nanodiscs composed of DMPC, cholesterol-containing nanodiscs, and cationic-lipid-containing nandiscs effectively remodeled plasma HDL. Nanodiscs composed of DPPC and DSPC showed little to no remodeling when incubated with human plasma. This differential remodeling capacity seems to be in line with the two-phase model, in which lipids are organized into a core and a boundary with distinct phase properties and

accessibility. The effective remodeling by DMPC-22A nanodiscs could result from the nanodiscs' inherent high fluidity at physiological temperatures, as suggested by their low main phase transition temperature of 24 degrees. At physiological temperature, both the boundary and core lipids in DMPC-22A nanodiscs could largely be in a fluid-like phase, facilitating the exchange of protein and phospholipid components necessary for remodeling interactions. The lack of remodeling by DPPC-22A and DSPC-22A nanodiscs could be attributed to their high main phase transition temperature. Despite the boundary lipids being disordered by the 22A peptide, the core lipids in these nanodiscs remain predominantly in a rigid, gel-like phase at physiological temperatures, restricting lipid mobility and accessibility. The partial remodeling observed with nanodiscs composed of binary lipids with different main phase transition temperatures suggests that the collective physical properties of combined phospholipids can create intermediate fluidity patches that allow limited lipid and peptide exchange. It is also plausible that a heterogeneous population of lipid nanodiscs forms where the lipid ratio is not constant, and even almost pure DMPC, DPPC, or DSPC discs can exist in the mixture samples. Incorporation of cholesterol into nanodiscs such as DPPC-22A and DSPC-22A significantly promoted remodeling. Incorporation of cholesterol into nanodiscs induces ordering in the fluid phases, whereas it is known to incorporate into tightly packed, gel-like regions, increasing their disorder and mobility (Krause and Regen 2014; Martinez et al. 2017). Thus, cholesterol tends to move both the gel and the liquid-disordered phase towards a liquid-ordered phase with an intermediate degree of compactness, fluidity, and lateral mobility (Schachter et al. 2022). Nanodiscs containing cationic lipid (DMTAP) extensively remodeled plasma HDL regardless of the primary phospholipid content. This emphasizes the impact of electrostatic interactions with negatively charged components on the surface of plasma HDL particles. Thus, even if the core of nanodiscs were to adopt a more rigid, gel-like phase, as may be the case for DPPC and DSPC, electrostatic effects could override these limitations and potentially promote fusion, thereby facilitating lipid and protein exchange. In addition, human plasma high-density lipoproteins (HDL2 and HDL3) as well as nanodiscs composed of DMPC and peptide 4F are known to exist in dynamic equilibrium (Grow and Fried 1978; Ravula et

al. 2018). Wool et al. (2009) reported that the apoA-I mimetic peptide L4F localized mainly with the HDL fraction upon incubation with human plasma. Since both HDL and nanodiscs exist in dynamic equilibrium, and it is known that apoA-I mimetics have a higher affinity for HDL, it is possible that they fuse when incubated together, particularly if the nanodiscs are largely in liquid-ordered or disordered phases. This results in the formation of pre-β HDL and lipid-poor apoA-I, as seen in Figure 4.

To conclude, we successfully demonstrated the critical interplay between the physicochemical parameters of phospholipids, their unique phase transition behaviour, and the dynamic gel and fluid states within the nanodiscs. Specifically, our findings show that acyl chain length, the combined properties of phospholipids, and the incorporation of cholesterol or cationic lipids are key determinants of size, electrostatic interactions, fluidity, and, hence, remodeling capacity. While the present findings offer significant insights into optimizing lipid components to achieve desired functional outcomes, certain limitations of the current study need to be acknowledged. Recognizing these limitations paves the way for future research to optimize nanodisc formulation and its therapeutic applications. One limitation of this study is that cryo-EM was performed on only a single sHDL formulation. This limits our understanding of particle morphology (shape and size) across different compositions, making it challenging to correlate particle morphology with remodeling efficiency. Functional studies, such as a cholesterol efflux assay, were not carried out. These assays provide evidence of sHDL particle activity and would allow us to quantify how efficiently different formulations promote HDL remodeling. In addition, the molecular mechanisms underlying HDL remodeling were not investigated. Molecular dynamics simulations were not performed, which could have complemented the experimental data by providing detailed insights into lipid and peptide behaviour at the molecular level, thereby helping predict particle stability, fluidity, and remodeling potential. Furthermore, in vivo studies were not conducted, leaving essential parameters such as circulation time, protein corona formation, plasma stability, and interactions with physiological components unexplored. Addressing these limitations in future research by combining comprehensive structural characterization, functional assays, mechanistic studies, computational modeling, and in vivo evaluation

could provide a more complete understanding of sHDL behaviour and allow the design of nanodiscs with optimized properties. One possibility for future research is to design sHDL formulations that do not remodel plasma HDL and can instead deliver cargo to targeted sites, such as liver X receptor agonists to atherosclerotic plaques. This could be achieved by incorporating anionic or PEGylated lipids to modulate particle interactions, enhance stability, and extend circulation time under physiological conditions.

Building on these findings and addressing these limitations, future research that integrates structural, functional, and in vivo studies could transform sHDL nanoparticles from experimental in vitro models into viable, innovative therapeutic tools for treating cardiovascular disease.

5. Acknowledgements

I would like to express my sincere gratitude to my supervisor, Artturi Koivuniemi, for his invaluable guidance, encouragement, and support throughout this work. He allowed me to work independently in the laboratory while always helping me clarify my questions and concepts, which greatly enhanced my understanding and confidence as a researcher. I also thank the DDCB Unit at the Faculty of Pharmacy, University of Helsinki, supported by HiLIFE and Biocenter Finland, for providing access to facilities. The facilities and expertise of the HiLIFE Cryo-EM unit at the University of Helsinki, members of Instruct-ERIC Centre Finland, FINStruct, and Biocenter Finland, are gratefully acknowledged. Finally, I wish to acknowledge all my laboratory colleagues for their insightful discussions and technical assistance, which greatly contributed to the completion of this thesis.

6. References

1. Ajoolabady A, Pratico D, Lin L, et al (2024) Inflammation in atherosclerosis: pathophysiology and mechanisms. Cell Death & Disease 2024 15:11 15:817-. https://doi.org/10.1038/s41419-024-07166-8
2. Alexander ET, Vedhachalam C, Sankaranarayanan S, et al (2010) Influence of ApoA-I Domain Structure on Macrophage Reverse Cholesterol Transport in Mice. Arterioscler Thromb Vasc Biol 31:320. https://doi.org/10.1161/ATVBAHA.110.216226
3. Aprotosoaie AC, Costache AD, Costache II (2022) Therapeutic Strategies and Chemoprevention of Atherosclerosis: What Do We Know and Where Do We Go? Pharmaceutics 14:722. https://doi.org/10.3390/PHARMACEUTICS14040722
4. Bandeali S, Farmer J (2012) High-density lipoprotein and atherosclerosis: The role of antioxidant activity. Curr Atheroscler Rep 14:101–107. https://doi.org/10.1007/S11883-012-0235-2
5. Bashir B, Schofield J, Downie P, et al (2024) Beyond LDL-C: unravelling the residual atherosclerotic cardiovascular disease risk landscape—focus on hypertriglyceridaemia. Front Cardiovasc Med 11:1389106. https://doi.org/10.3389/FCVM.2024.1389106
6. Bourdi M, Amar M, Remaley AT, Terse PS (2018) Intravenous toxicity and toxicokinetics of an HDL mimetic, Fx-5A peptide complex, in cynomolgus monkeys. Regulatory Toxicology and Pharmacology 100:59–67. https://doi.org/10.1016/J.YRTPH.2018.10.009
7. Cañ O, Casals C (2013) Differential Scanning Calorimetry of Protein-Lipid Interactions. https://doi.org/10.1007/978-1-62703-275-9_4
8. Cascajo-Castresana M, David RO, Iriarte-Alonso MA, et al (2020) Protein aggregates nucleate ice: The example of apoferritin. Atmos Chem Phys 20:3291–3315. https://doi.org/10.5194/ACP-20-3291-2020
9. Casula M, Colpani O, Xie S, et al (2021) HDL in Atherosclerotic Cardiovascular Disease: In Search of a Role. Cells 2021, Vol 10, Page 1869 10:1869. https://doi.org/10.3390/CELLS10081869

10. Chakraborty S, Doktorova M, Molugu TR, et al (2020) How cholesterol stiffens unsaturated lipid membranes. Proc Natl Acad Sci U S A 117:21896–21905. https://doi.org/10.1073/PNAS.2004807117
11. Chen W, Duša F, Witos J, et al (2018) Determination of the Main Phase Transition Temperature of Phospholipids by Nanoplasmonic Sensing. Scientific Reports 2018 8:1 8:14815-. https://doi.org/10.1038/s41598-018-33107-5
12. Denisov IG, McLean MA, Shaw AW, et al (2005) Thermotropic phase transition in soluble nanoscale lipid bilayers. J Phys Chem B 109:15580. https://doi.org/10.1021/JP051385G
13. Di Bartolo BA, Nicholls SJ, Bao S, et al (2011) The apolipoprotein A-I mimetic peptide ETC-642 exhibits anti-inflammatory properties that are comparable to high density lipoproteins. Atherosclerosis 217:395–400. https://doi.org/10.1016/J.ATHEROSCLEROSIS.2011.04.001
14. Drabik D, Chodaczek G, Kraszewski S, Langner M (2020) Mechanical Properties Determination of DMPC, DPPC, DSPC, and HSPC Solid-Ordered Bilayers. Langmuir 36:3826–3835. https://doi.org/10.1021/ACS.LANGMUIR.0C00475
15. Durowoju IB, Bhandal KS, Hu J, et al (2017) Differential Scanning Calorimetry — A Method for Assessing the Thermal Stability and Conformation of Protein Antigen. J Vis Exp 2017:55262. https://doi.org/10.3791/55262
16. Fan J, Watanabe T (2022) Atherosclerosis: Known and unknown. Pathol Int 72:151–160. https://doi.org/10.1111/PIN.13202
17. Fawaz M V, Kim SY, Li D, et al (2020) Phospholipid Component Defines Pharmacokinetic and Pharmacodynamic Properties of Synthetic High-Density Lipoproteins s. THE JOURNAL OF PHARMACOLOGY AND EXPERIMENTAL THERAPEUTICS J Pharmacol Exp Ther 372:193–204. https://doi.org/10.1124/jpet.119.257568
18. Gantt E (1969) Properties and Ultrastructure of Phycoerythrin From Porphyridium cruentum. Plant Physiol 44:1629. https://doi.org/10.1104/PP.44.11.1629
19. Grow TE, Fried M (1978) Interchange of apoprotein components between the human plasma high density lipoprotein subclasses HDL2 and HDL3 in vitro. Journal of

Biological Chemistry 253:8034–8041. https://doi.org/10.1016/S0021-9258(17)34357-0

20. Hartkamp R, Moore TC, Iacovella CR, et al (2016) Investigating the Structure of Multicomponent Gel-Phase Lipid Bilayers. Biophys J 111:813–823. https://doi.org/10.1016/J.BPJ.2016.07.016
21. Hetherington I, Totary-Jain H (2022) Anti-atherosclerotic therapies: Milestones, challenges, and emerging innovations. Molecular Therapy 30:3106–3117. https://doi.org/10.1016/j.ymthe.2022.08.024
22. Hung WC, Lee MT, Chen FY, Huang HW (2007) The Condensing Effect of Cholesterol in Lipid Bilayers. Biophys J 92:3960. https://doi.org/10.1529/BIOPHYSJ.106.099234
23. Jakubec M, Bariås E, Furse S, et al (2021) Cholesterol-containing lipid nanodiscs promote an α-synuclein binding mode that accelerates oligomerization. FEBS J 288:1887–1905. https://doi.org/10.1111/FEBS.15551
24. Risselda HJ, Marrink SJ (2009) Curvature effects on lipid packing and dynamics in liposomes revealed by coarse grained molecular dynamics simulations. Physical Chemistry Chemical Physics 11:2056–2067. https://doi.org/10.1039/B818782G
25. Johansen NT, Luchini A, Tidemand FG, et al (2021) Structural and Biophysical Properties of Supercharged and Circularized Nanodiscs. Langmuir 37:6681–6690. https://doi.org/10.1021/ACS.LANGMUIR.1C00560
26. Keene D, Price C, Shun-Shin MJ, Francis DP (2014) Effect on cardiovascular risk of high density lipoprotein targeted drug treatments niacin, fibrates, and CETP inhibitors: meta-analysis of randomised controlled trials including 117 411 patients. BMJ 349:. https://doi.org/10.1136/BMJ.G4379
27. Khodadadi E, Khodadadi E, Chaturvedi P, Moradi M (2025) Comprehensive Insights into the Cholesterol-Mediated Modulation of Membrane Function Through Molecular Dynamics Simulations. Membranes (Basel) 15:173. https://doi.org/10.3390/MEMBRANES15060173
28. Kim SY, Kang J, Fawaz M V., et al (2023) Phospholipids impact the protective effects of HDL-mimetic nanodiscs against lipopolysaccharide-induced inflammation. Nanomedicine 18:2127–2142. https://doi.org/10.2217/NNM-2023-0222

29. Kleinauskaite G (2025) Characterization and Functional Assessment of High-Density Lipoprotein Mimetic Nanodiscs Comprised of Different Apolipoprotein A-I mimetic Peptides and Phospholipids (Master Thesis) University of Helsinki
30. Kowara M, Cudnoch-Jedrzejewska A (2021) Pathophysiology of Atherosclerotic Plaque Development-Contemporary Experience and New Directions in Research. International Journal of Molecular Sciences 2021, Vol 22, Page 3513 22:3513. https://doi.org/10.3390/IJMS22073513
31. Krause MR, Regen SL (2014) The structural role of cholesterol in cell membranes: From condensed bilayers to lipid rafts. Acc Chem Res 47:3512–3521. https://doi.org/10.1021/AR500260T
32. Krishnarjuna B, Anantharamaiah GM, Ramamoorthy A (2025) Peptide nanodiscs: Versatile platforms for membrane protein functional reconstitution and structural studies: A review. Int J Biol Macromol 333:148668. https://doi.org/10.1016/J.IJBIOMAC.2025.148668
33. Kuai R, Subramanian C, White PT, et al (2017) synthetic high-density lipoprotein nanodisks for targeted withalongolide delivery to adrenocortical carcinoma. Int J Nanomedicine 12–6581. https://doi.org/10.2147/IJN.S140591
34. López CA, Swift MF, Xu XP, et al (2019) Biophysical Characterization of a Nanodisc with and without BAX: An Integrative Study Using Molecular Dynamics Simulations and Cryo-EM. Structure 27:988-999.e4. https://doi.org/10.1016/J.STR.2019.03.013
35. Lyu D, Zhang L, Zhang Y (2020) Effects of cholesterol on bilayers with various degrees of unsaturation of their phospholipid tails under mechanical stress. RSC Adv 10:11088. https://doi.org/10.1039/D0RA00624F
36. Mabrey S, Sturtevant JM (1976) Investigation of phase transitions of lipids and lipid mixtures by high sensitivity differential scanning calorimetry. Proc Natl Acad Sci U S A 73:3862–3866. https://doi.org/10.1073/PNAS.73.11.3862
37. Madaudo C, Bono G, Ortello A, et al (2024) Dysfunctional High-Density Lipoprotein Cholesterol and Coronary Artery Disease: A Narrative Review. Journal of Personalized Medicine 2024, Vol 14, Page 996 14:996. https://doi.org/10.3390/JPM14090996

38. Mahmood T, Shapiro MD (2021) The Questions on Everyone's Mind: What is and Why Do We Need Preventive Cardiology? Methodist Debakey Cardiovasc J 17:8. https://doi.org/10.14797/MDCVJ.698
39. Marques LR, Diniz TA, Antunes BM, et al (2018) Reverse cholesterol transport: Molecular mechanisms and the non-medical approach to enhance HDL cholesterol. Front Physiol 9:331734. https://doi.org/10.3389/FPHYS.2018.00526
40. Martinez D, Decossas M, Kowal J, et al (2017) Lipid Internal Dynamics Probed in Nanodiscs. Chemphyschem 18:2651. https://doi.org/10.1002/CPHC.201700450
41. Miyazaki M, Tajima Y, Ishihama Y, et al (2013) Effect of phospholipid composition on discoidal HDL formation. Biochimica et Biophysica Acta (BBA) - Biomembranes 1828:1340–1346. https://doi.org/10.1016/J.BBAMEM.2013.01.012
42. Nankar SA, Kawathe PS, Abhay ·, Pande H (2022) HDL, ApoA-I and ApoE-Mimetic Peptides: Potential Broad Spectrum Agent for Clinical Use? Int J Pept Res Ther 28:52. https://doi.org/10.1007/s10989-021-10352-3
43. Nicholls SJ, Andrews J, Kastelein JJP, et al (2018a) Effect of Serial Infusions of CER-001, a Pre-β High-Density Lipoprotein Mimetic, on Coronary Atherosclerosis in Patients Following Acute Coronary Syndromes in the CER-001 Atherosclerosis Regression Acute Coronary Syndrome Trial: A Randomized Clinical Trial. JAMA Cardiol 3:815. https://doi.org/10.1001/JAMACARDIO.2018.2121
44. Nicholls SJ, Puri R, Ballantyne CM, et al (2018b) Effect of Infusion of High-Density Lipoprotein Mimetic Containing Recombinant Apolipoprotein A-I Milano on Coronary Disease in Patients With an Acute Coronary Syndrome in the MILANO-PILOT Trial: A Randomized Clinical Trial. JAMA Cardiol 3:806. https://doi.org/10.1001/JAMACARDIO.2018.2112
45. Nouri S, Niemelä A, Nencini R, et al (2025) Exploring Peptide Nanodiscs Structure and Dynamics through Synergistic Approach of NMR Spectroscopy, SAS and MD Simulations. bioRxiv 2025.09.02.673616. https://doi.org/10.1101/2025.09.02.673616

46. Ouimet M, Barrett TJ, Fisher EA (2019) HDL and reverse cholesterol transport: Basic mechanisms and their roles in vascular health and disease. Circ Res 124:1505–1518. https://doi.org/10.1161/CIRCRESAHA.119.312617
47. Pahwa R, Jialal I. (2023). Atherosclerosis. In StatPearls (internet). https://www.ncbi.nlm.nih.gov/books/NBK507799/
48. Pan J, Mills TT, Tristram-Nagle S, Nagle JF (2008) Cholesterol perturbs lipid bilayers nonuniversally. Phys Rev Lett 100:198103. https://doi.org/10.1103/PHYSREVLETT.100.198103
49. Pasti A Pietro, Rossi V, Di Stefano G, et al (2022) Human lactate dehydrogenase A undergoes allosteric transitions under pH conditions inducing the dissociation of the tetrameric enzyme. Biosci Rep 42:BSR20212654. https://doi.org/10.1042/BSR20212654
50. Patel H, Ding B, Ernst K, et al (2019) Characterization of apolipoprotein A-I peptide phospholipid interaction and its effect on HDL nanodisc assembly. Int J Nanomedicine 14:3069–3086. https://doi.org/10.2147/IJN.S179837
51. Phillips MC (2013) New insights into the determination of HDL structure by apolipoproteins: Thematic Review Series: High Density Lipoprotein Structure, Function, and Metabolism. J Lipid Res 54:2034–2048. https://doi.org/10.1194/JLR.R034025
52. Poznyak A V., Sadykhov NK, Kartuesov AG, et al (2022) Hypertension as a risk factor for atherosclerosis: Cardiovascular risk assessment. Front Cardiovasc Med 9:959285. https://doi.org/10.3389/FCVM.2022.959285
53. Puthenveetil R, Nguyen K, Vinogradova O (2016) Nanodiscs and Solution NMR: preparation, application and challenges. Nanotechnol Rev 6:111. https://doi.org/10.1515/NTREV-2016-0076
54. Rani A, Marsche G (2023) A Current Update on the Role of HDL-Based Nanomedicine in Targeting Macrophages in Cardiovascular Disease. Pharmaceutics 15:1504. https://doi.org/10.3390/PHARMACEUTICS15051504

55. Ravula T, Ishikuro D, Kodera N, et al (2018) Real-Time Monitoring of Lipid Exchange via Fusion of Peptide Based Lipid-Nanodiscs. Chemistry of Materials 30:3204–3207. https://doi.org/10.1021/ACS.CHEMMATER.8B00946
56. Riaz H, Khan SU, Lateef N, et al (2019) Residual inflammatory risk after contemporary lipid lowering therapy. Eur Heart J Qual Care Clin Outcomes 6:105. https://doi.org/10.1093/EHJQCCO/QCZ055
57. Ronsein GE, Vaisar T (2017) Inflammation, Remodeling and Other Factors Affecting HDL Cholesterol Efflux. Curr Opin Lipidol 28:52. https://doi.org/10.1097/MOL.0000000000000382
58. Rye KA, Bursill CA, Lambert G, et al (2009) The metabolism and anti-atherogenic properties of HDL. J Lipid Res 50:S195–S200. https://doi.org/10.1194/JLR.R800034-JLR200
59. Schachter I, Paananen RO, Fábián B, et al (2022) The Two Faces of the Liquid Ordered Phase. Journal of Physical Chemistry Letters 13:1307–1313. https://doi.org/10.1021/ACS.JPCLETT.1C03712
60. Schwendeman A, Sviridov DO, Yuan W, et al (2015) The effect of phospholipid composition of reconstituted HDL on its cholesterol efflux and anti-inflammatory properties. J Lipid Res 56:1727–1737. https://doi.org/10.1194/JLR.M060285
61. Sparks DL, Chatterjee C, Young E, et al (2008) Lipoprotein charge and vascular lipid metabolism. Chem Phys Lipids 154:1–6. https://doi.org/10.1016/J.CHEMPHYSLIP.2008.04.006
62. Sparr E, Hallin L, Markova N, Wennerström H (2002) Phospholipid-Cholesterol Bilayers under Osmotic Stress. Biophys J 83:2015–2025. https://doi.org/10.1016/S0006-3495(02)73963-5
63. Stepien P, Augustyn B, Poojari C, et al (2020) Complexity of seemingly simple lipid nanodiscs. Biochimica et Biophysica Acta (BBA) - Biomembranes 1862:183420. https://doi.org/10.1016/J.BBAMEM.2020.183420
64. Tang J, Li D, Drake L, et al (2017) Influence of route of administration and lipidation of apolipoprotein A-I peptide on pharmacokinetics and cholesterol mobilization. J Lipid Res 58:124–136. https://doi.org/10.1194/JLR.M071043

65. Trajkovska KT, Topuzovska S (2017) High-density lipoprotein metabolism and reverse cholesterol transport: strategies for raising HDL cholesterol. Anatol J Cardiol 18:149. https://doi.org/10.14744/ANATOLJCARDIOL.2017.7608
66. van Trier TJ, Mohammadnia N, Snaterse M, et al (2021) Lifestyle management to prevent atherosclerotic cardiovascular disease: evidence and challenges. Netherlands Heart Journal 30:3. https://doi.org/10.1007/S12471-021-01642-Y
67. Wadsäter M, Maric S, Simonsen JB, et al (2013) The effect of using binary mixtures of zwitterionic and charged lipids on nanodisc formation and stability. Soft Matter 9:2329–2337. https://doi.org/10.1039/C2SM27000E
68. Wang B, Tieleman DP (2024) The structure, self-assembly and dynamics of lipid nanodiscs revealed by computational approaches. Biophys Chem 309:107231. https://doi.org/10.1016/J.BPC.2024.107231
69. Wang Z, He X, Bai H, et al (2025) Recent progress in anti-atherosclerosis strategies and prospective therapeutic targets. Int J Pharm 684:126122. https://doi.org/10.1016/J.IJPHARM.2025.126122
70. Werba JP, Vigo LM, Veglia F, et al (2019) Trials in “True” Dyslipidemic Patients Are Urged to Reconsider Comprehensive Lipid Management as a Means to Reduce Residual Cardiovascular Risk. Clin Pharmacol Ther 106:960. https://doi.org/10.1002/CPT.1436
71. Wool GD, Vaisar T, Reardon CA, Getz GS (2009) An apoA-I mimetic peptide containing a proline residue has greater in vivo HDL binding and anti-infl ammatory ability than the 4F peptide. J Lipid Res 50:. https://doi.org/10.1194/jlr.M900151-JLR200
72. Yohannes G, Wiedmer SK, Elomaa M, et al (2010) Thermal aggregation of bovine serum albumin studied by asymmetrical flow field-flow fractionation. Anal Chim Acta 675:191–198. https://doi.org/10.1016/J.ACA.2010.07.016
73. You X, Thakur N, Ray AP, et al (2022) A comparative study of interfacial environments in lipid nanodiscs and vesicles. Biophysical Reports 2:100066. https://doi.org/10.1016/J.BPR.2022.100066

74. Yu M, Hong K, Adili R, et al (2022) Development of activated endothelial targeted high-density lipoprotein nanoparticles. Front Pharmacol 13:902269. https://doi.org/10.3389/FPHAR.2022.902269
75. Yuan W, Ernst K, Kuai R, et al (2023) Systematic evaluation of the effect of different apolipoprotein A-I mimetic peptides on the performance of synthetic high-density lipoproteins in vitro and in vivo. Nanomedicine 48:102646. https://doi.org/10.1016/J.NANO.2022.102646
76. Zhao Y, Imura T, Leman LJ, et al (2013) Mimicry of High-Density Lipoprotein: Functional Peptide–Lipid Nanoparticles Based on Multivalent Peptide Constructs. J Am Chem Soc 135:10.1021/ja404714a. https://doi.org/10.1021/JA404714A